Transient p53 suppression increases reprogramming of human fibroblasts without affecting apoptosis and DNA damage

Rasmussen, Mikkel Aabech; Holst, Bjørn; Tümer, Zeynep; Johnsen, Mads G.; Zhou, Shuling; Stummann, Tina C.; Hyttel, Poul; Clausen, Christian

Stem Cell Reports

Report

ISSCR

OPEN ACCESS

Transient p53 Suppression Increases Reprogramming of Human Fibroblasts without Affecting Apoptosis and DNA Damage

Mikkel A. Rasmussen,[1,*] Bjørn Holst,[2] Zeynep Tümer,[3] Mads G. Johnsen,[2] Shuling Zhou,[1] Tina C. Stummann,[4] Poul Hyttel,[1] and Christian Clausen[2]

[1]Department of Veterinary Clinical and Animal Sciences, Faculty of Health and Medical Sciences, University of Copenhagen, Groennegaardsvej 7, Frederiksberg C 1870, Denmark
[2]Bioneer A/S, Kogle Alle 2, Hoersholm 2970, Denmark
[3]Applied Human Molecular Genetics, Kennedy Center, Copenhagen University Hospital, Rigshospitalet, Gl. Landevej 7, Glostrup 2600, Denmark
[4]H. Lundbeck A/S, Ottiliavej 9, Valby 2500, Denmark
*Correspondence: mar@bioneer.dk
 http://dx.doi.org/10.1016/j.stemcr.2014.07.006
This is an open access article under the CC BY-NC-ND license (http://creativecommons.org/licenses/by-nc-nd/3.0/).

SUMMARY

The discovery of human-induced pluripotent stem cells (iPSCs) has sparked great interest in the potential treatment of patients with their own in vitro differentiated cells. Recently, knockout of the Tumor Protein 53 (p53) gene was reported to facilitate reprogramming but unfortunately also led to genomic instability. Here, we report that transient suppression of p53 during nonintegrative reprogramming of human fibroblasts leads to a significant increase in expression of pluripotency markers and overall number of iPSC colonies, due to downstream suppression of p21, without affecting apoptosis and DNA damage. Stable iPSC lines generated with or without p53 suppression showed comparable expression of pluripotency markers and methylation patterns, displayed normal karyotypes, contained between 0 and 5 genomic copy number variations and produced functional neurons in vitro. In conclusion, transient p53 suppression increases reprogramming efficiency without affecting genomic stability, rendering the method suitable for in vitro mechanistic studies with the possibility for future clinical translation.

INTRODUCTION

Dr. Wilmut and colleague's discovery in 1996 that mammalian somatic cells can be reprogrammed into a totipotent state of development by fusion with an enucleated oocyte (Campbell et al., 1996) has paved the way for autologous stem cell therapy by exploiting a patient's own in vitro differentiated cells. Ten years later, with the revolutionizing finding that induced pluripotent stem cells (iPSCs) can be established from somatic cells by overexpression of merely four transcription factors (Takahashi and Yamanaka, 2006), a major step toward a clinical translation was taken. However, new coding mutations were recently reported to arise during the reprogramming process (Gore et al., 2011; Laurent et al., 2011; Martins-Taylor and Xu, 2012; Ng et al., 2011), rendering the process too hazardous for regenerative use in humans.

Several nonintegrative reprogramming strategies including Sendai virus (Fusaki et al., 2009) and episomal plasmids (Okita et al., 2011, 2013; Yu et al., 2009) have been tested to produce safe, transplantable iPSCs. Yet, recent whole-genome sequencing studies have failed to demonstrate a reduction in the mutational load in iPSC lines derived by integration-free reprogramming methods (Gore et al., 2011).

The cell-cycle regulator p53 acts as an important safeguard mechanism, by preventing cells from undergoing uncontrolled proliferation in response to DNA damage (Hong et al., 2009). The downstream DNA damage response (DDR) involves a series of events that lead to either cell-cycle arrest induced by p21 or apoptosis induced by PUMA. Importantly, p53 has also been shown to act as a critical barrier to the reprogramming process, and knockout of the TP53 gene in mouse and human fibroblasts was shown to produce significantly more iPSC colonies (Hong et al., 2009; Kawamura et al., 2009; Marión et al., 2009). Although the inhibition of p53 is clearly advantageous for the reprogramming efficiency, knocking out TP53 may possess critical safety issues because it was found to cause genomic instability (Chen et al., 2012; Lake et al., 2012; Marión et al., 2009; Menendez et al., 2010).

Recently, transient suppression of p53 with nonintegrative plasmids was shown to improve the reprogramming efficiency of human fibroblasts (Okita et al., 2011) and blood cells (Okita et al., 2013) by use of nonintegrative plasmids. Yet it remains unknown whether transient suppression of p53 will also give rise to genomic instability, which may in turn have detrimental effects on the gene expression, the epigenetic status, and the differentiation capacity of the resulting iPSC lines.

In this study, we set out to establish an optimized nonintegrative reprogramming approach under defined conditions in order to study the functional effects of transient p53 suppression in normal human dermal fibroblasts (NHDFs) during and after reprogramming.

RESULTS

Increased Reprogramming Efficiency with Transient p53 Suppression

To study the effect of transient p53 suppression during reprogramming of human fibroblasts, a nonintegrative reprogramming system was established in defined conditions (Figure 1A and Figure S1 available online). Seven days after reprogramming with or without (w/wo) transient expression of a short hairpin to *TP53* (shp53), a subpopulation of small, highly proliferative cells was observed in both conditions (Figures 1B and 1F). At days 14–28, iPSC colonies were observed (Figures 1C, 1D, 1G, and 1H), which stained positive for TRA-1-81 (Figures 1E and 1I). The growth rate was, in general, higher during reprogramming with transient p53 suppression (0.12 cell doublings per day) compared to without (0.06 cell doublings per day), although not to a significant degree (Figure 1J). In contrast, a fibroblast line, which stably express shp53 (PLK.O; Godar et al., 2008) displayed a significantly higher growth rate (0.42 cell doublings per day), yet, this line proved resistant to reprogramming (data not shown). Alkaline phosphatase staining and counting on day 28 showed a significant (7.5-fold) increase in the number of iPSC colonies with transient p53 suppression (0.12%) compared to without (0.016%) (Figure 1K), which was confirmed in several independent experiments comprising NHDFs from different individuals.

Transient p53 Suppression Increases Reprogramming Efficiency through Inhibition of p21 without Affecting Apoptosis and DNA Damage

To investigate the underlying effect of the increased reprogramming efficiency with transient p53 suppression, temporal changes in pluripotency markers (SSEA4, TRA1-60), tumor suppression (p53), cell-cycle regulation (p21), apoptosis (PUMA), and DNA damage (H2A.X) were studied by flow cytometry. Although the PLK.O line stably expressing shp53 showed a 43.6% reduction in p53-positive cells compared to NHDFs, the pluripotency markers SSEA4 and TRA1-60 remained low during the entire reprogramming experiment (data not shown). In contrast, the analyses revealed a significant increase in SSEA4 and TRA1-60 double-positive cells with transient p53 suppression on day 21 (10.0% versus 3.1%) and on day 28 (16.6% versus 8.3%) after reprogramming (Figure 2A). A significant decrease in p53-positive cells was also observed with transient p53 suppression at days 7 (82.8% versus 90%), 14 (79% versus 92.7%), and 21 (63.8% versus 89.4%) (Figure 2B), which correlated with a significant decrease in p21-positive cells at days 7 (92.6% versus 96.3%), 14 (87.9% versus 95.6%), and 21 (68.1% versus 93.4%) (Figure 2C). In contrast, no significant effect of transient p53 suppression on apoptosis was observed, as evaluated by the proapoptotic marker PUMA (Figure 2D), a mitochondrial membrane assay (Figure S2A), and Annexin V in TRA1-60-positive cells (Figure S2B). Moreover, analysis with H2A.X, which is associated with replication-induced DNA damage (Garcia-Canton et al., 2012), detected no significant effect of transient p53 suppression on DNA damage, neither in the total cell population (Figure 2E) nor in TRA1-60-positive cells (Figures S2C and S2D).

Next, gene expression analysis of *TP53* and its downstream DDR targets *P21* and *PUMA*, as well as the pluripotency marker *NANOG* was performed. The silencing effect of shp53 resulted in a significant decrease in *TP53* expression in unsorted cells 7 days after reprogramming (Figure S2E), and in *P21* expression 14 days after reprogramming (Figure S2F), whereas expression of *PUMA* was unaffected (Figure S2G). In addition, no significant effect of shp53 suppression in TRA1-60-sorted cells was observed (Figures S2I–S2K). In contrast, the pluripotency marker *NANOG* was significantly upregulated in both unsorted and sorted cells 21 and 14 days after reprogramming with shp53, respectively (Figures S2H and S2L).

iPSCs Generated by Transient p53 Suppression Display Normal In Vitro Characteristics

To examine whether transient p53 suppression confers a negative effect on the long-term stability, six iPSC lines established w/wo transient p53 suppression were characterized in detail. Overall, there were no differences in morphology (Figures 3A and 3E). The pluripotency markers OCT4, NANOG, SSEA3, SSEA4, TRA1-60, and TRA1-81 were all detected by immunocytochemical staining (Figures 3B–3D and 3F–3H) and quantitative real-time PCR analyses showed a comparable upregulation of *POU5F1* (*OCT4*), *SOX2*, *NANOG*, *ZFP42*, *DNMT3B*, and *TP53* and downregulation of *P21* compared with NHDFs (Figure 3I). Moreover, integration analyses confirmed lack of expression from exogenous genes (Figure S3A). A comparable hypomethylation of the pluripotency-associated genes *OCT4*, *NANOG*, *SALL4*, and *RAB25* and hypermethylation of the fibroblast-associated gene *UBE1L* was also observed (Figure 3J). Genome-wide transcriptome profiling showed no significant up- or downregulated genes in iPSC lines generated w/wo transient p53 suppression and analysis with PluriTest showed that all iPSC lines scored within the predefined pluripotency and novelty scores (Figure 3K). Finally, in vitro differentiation confirmed by the ability to generate embryoid bodies (Figures 3L, 3M, 3P, and 3Q), which stained positive for Beta-III-tubulin (TUJI) (Figures 3N and 3R), smooth muscle actin (SMA), and alpha-fetoprotein (AFP) (Figures 3O and 3S).
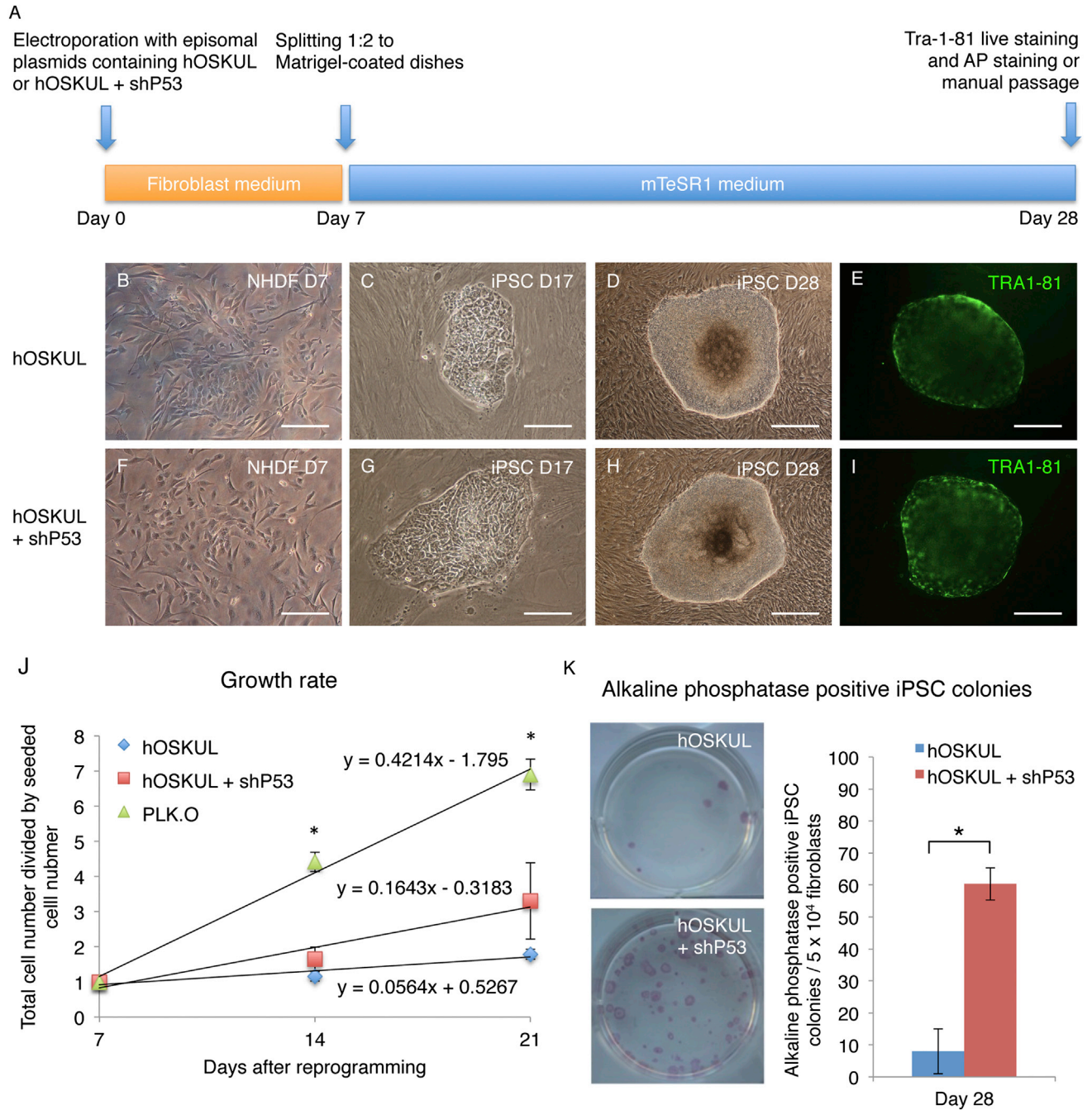
Figure 1. Increased Reprogramming with Transient p53 Suppression in Defined Conditions

(A) Timeline showing the reprogramming in defined conditions with the episomal plasmids *hOCT4*, *hSOX2*, *hKLF4*, *hL-MYC*, and *hLIN28* (hOSKUL) with or without (w/wo) a short hairpin to p53 (shp53).

(B–D and F–H) Morphology of normal human dermal fibroblasts (NHDFs) and induced pluripotent stem cells (iPSCs) at days 7, 17, and 28 after reprogramming w/wo shp53.

(E and I) Tra-1-81 staining of primary iPSC colonies 28 days after reprogramming w/wo shp53.

(J) Growth rate of cells electroporated with hOSKUL, hOSKUL + shp53, or a fibroblast line stably expressing shp53 (PLK.O) at days 7, 21, and 28 after reprogramming.

(K) Alkaline phosphatase staining and counting of primary iPSC colonies at day 28 after reprogramming w/wo shp53.

Scale bars, 200 μm (B, C, F, and G) and 400 μm (D, E, H, and I). Y error bars depict SD of three independent experiments. *p < 0.05. See also Figure S1.
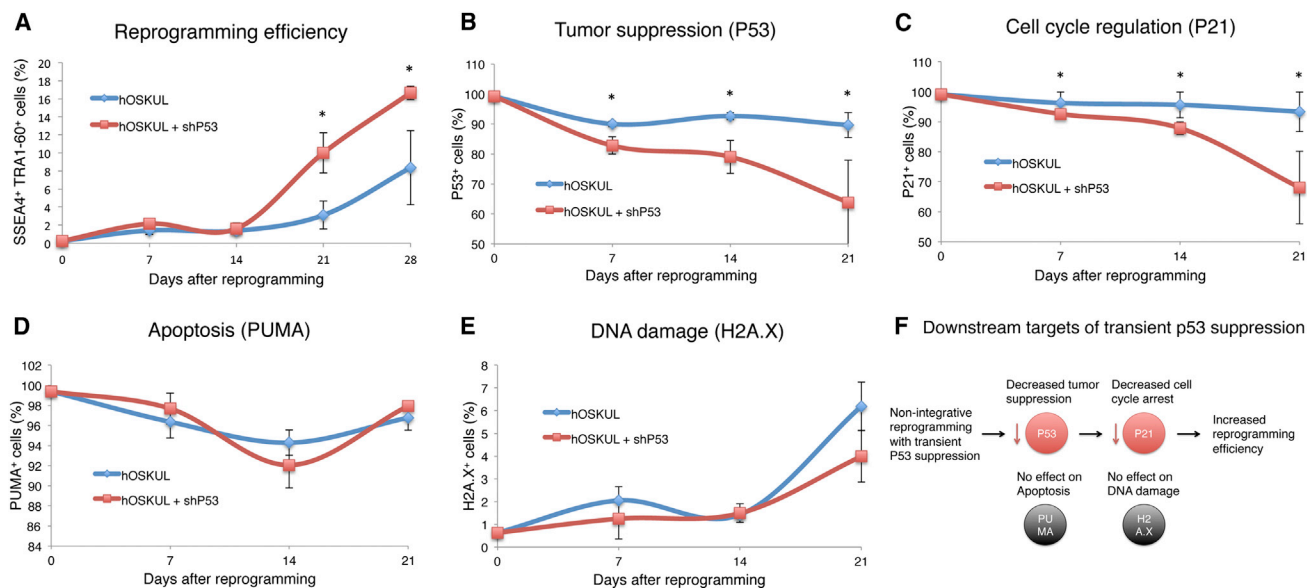
Figure 2. Transient p53 Suppression Increases Reprogramming Efficiency without Affecting Apoptosis and DNA Damage

Flow cytometry of normal human dermal fibroblasts (NHDFs) on days 0, 7, 14, 21, and 28 after reprogramming with the episomal plasmids *hOCT4*, *hSOX2*, *hKLF4*, *hL-MYC*, and *hLIN28* (hOSKUL) with or without (w/wo) a short hairpin to p53 (shp53).

(A–E) Flow cytometry was performed with (A) the pluripotency markers SSEA4 and TRA1-60, (B) the tumor suppressor p53, (C) the cell-cycle regulator p21, (D) the proapoptotic marker PUMA, and (E) the double-stranded DNA damage marker H2A.X.

(F) Overview depicting the mechanisms involved in transient p53 suppression during reprogramming. Y error bars depict SD of three independent experiments. *p < 0.05. See also Figure S2.

iPSCs Generated by Transient p53 Suppression Show Genomic Stability

The genomic stability of fibroblasts and iPSC lines generated w/wo transient p53 suppression was analyzed in detail by chromosome studies and copy number variation (CNV) analyses. All the lines presented normal karyotype and did not contain any microscopically visible structural or numerical abnormalities (46, XY) (Figure S3B). CNV analyses showed no significant differences between the numbers of CNVs in iPSC lines generated w/wo transient p53 suppression, displaying an average of 1.66 genomic CNVs (four gains and six losses), which were not present in the donor NHDFs (Table S1). Three of the CNVs were detected in iPSC lines without transient p53 suppression, with one line containing two CNVs (K1), one line containing a single CNV (K3), and one line containing no CNVs (K2). In contrast, seven of the CNVs were detected in iPSC lines with transient p53 suppression, with one line (K1_shp53) containing five CNVs, whereas the other two lines (K2_shp53 and K3_shp53) had only a single CNV each, the latter in a noncoding region.

iPSCs Generated by Transient p53 Suppression Can Differentiate to Functional Neurons In Vitro

To evaluate the differentiation potential of iPSC lines established w/wo transient p53 suppression, directed neural dif-

ferentiation was performed (Figure 4A). At day 12, all the iPSC lines had formed a uniform monolayer of tightly packed neuroepithelial cells (Figures 4B and 4F), and at days 21, a population of neural progenitor cells (NPCs) was formed, which stained positive for the NPC markers SOX2, NESTIN (Figures 4J and 4N), and VIMENTIN (Figures 4K and 4O), whereas OCT4 was negative. After subsequent culture and passage for 35 days, a network of neural structures was observed (Figures 4D and 4H), containing neurons with a bi- or multipolar morphology with long axonal connections (Figures 4E and 4I). At this stage, most of the cells stained positive for TUJI (Figures 4L and 4P) and the glutamatergic marker vGLUT (Figures 4M and 4Q). Functional characterization on day 80 showed that the iPSC lines responded to glutamate/glycine (Figures 4R and 4T), GABA, and acetylcholine (Figures 4S and 4U), indicating the presence of receptors for these neurotransmitters.
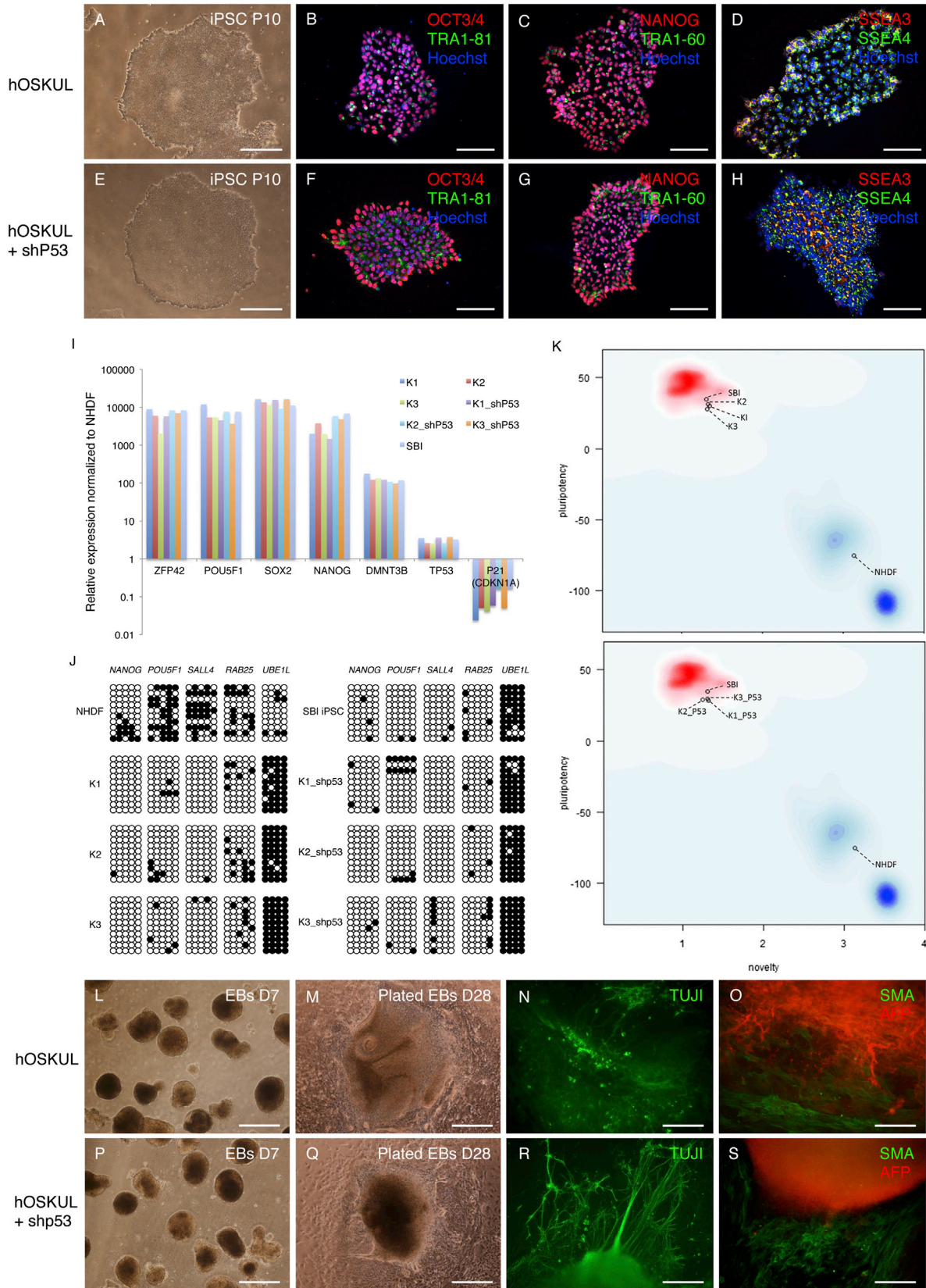
DISCUSSION

In this study, we report the establishment of a noninte-grative reprogramming approach in defined conditions, based on transient suppression of p53. Using this method, we were able to consistently generate AP and TRA1-81-positive iPSC colonies from individuals with

Stem Cell Reports

Effects of Transient p53 Suppression on Human iPSCs

(legend on next page)

different genders and ages. Compared to the results of Okita et al. (2011), who reported an average of 30 iPSC colonies per 1×10^5 human fibroblasts (0.03%), we observed a 3-fold increase (0.11%) at defined conditions. In contrast, a fibroblast line stably expressing shp53 did not produce any iPSC colonies, and it is likely that the uncontrolled growth of this line has made it resistant to reprogramming due to accumulation of DNA damage or severe shortening of telomeres.

To study temporal changes during reprogramming with transient p53 suppression, flow cytometry with the pluripotency markers SSEA4/TRA1-60, which were previously used for isolation of fully reprogrammed iPSCs (Kahler et al., 2013), was performed. A significant increase in the amount of SSEA4/TRA1-60 double-positive cells was observed on day 21 (3-fold) and on day 28 (2-fold) after reprogramming with shp53. Moreover, transient p53 suppression also accelerated the temporal appearance of fully reprogrammed iPSCs, as the cells became earlier positive for SSEA4/TRA1-60.

As expected from the silencing effect of shp53, p53 was significantly suppressed during reprogramming with transient p53 suppression, which correlated with suppression of p21, whereas expression of the proapoptotic marker PUMA remained unchanged. These results imply that transient p53 suppression increases reprogramming by activating cell proliferation through p21 suppression, rather than by decreasing apoptosis (Figure 2F). Moreover, the effect of transient p53 suppression appears to occur in fibroblasts prior to reprogramming, because no significant differences in TP53, P21, and PUMA were observed in TRA1-60-sorted cells (Figures S2I–S2L). The latter is in agreement with a recent study, which demonstrated that embryonic stem cells (ESCs) possess a nonfunctional p53-p21 axis, in which p53 activates specific microRNAs, which inhibit p21 expression, thereby affecting cell-cycle regulation (Dolezalova et al., 2012). In contrast, NANOG was up-

regulated with transient p53 suppression in both unsorted and TRA1-60-sorted cells; thus, NANOG could be a potential downstream target of p53. In addition, knockout of tp53 in mouse fibroblasts was recently shown to increase reprogramming through actions of p21 by promoting a mesenchymal-to-epithelial (MET) transition (Brosh et al., 2013), which could also apply in human.

Marión and colleagues previously reported that knockout of TP53 in human and mouse fibroblasts allows for efficient reprogramming at the expense of increased DNA damage, which was attributed to a decrease in apoptosis of DNA damaged cells (Marión et al., 2009). In contrast, we found that transient p53 suppression did not induce DNA damage or result in a decrease in apoptosis during reprogramming. The underlying mechanism is likely to constitute a combination of nonintegrative plasmids, which prevents excessive DNA damage, and a low background expression of TP53, which may be sufficient to sustain the apoptotic pathway.

To examine whether transient suppression of p53 had a negative effect on the long-term stability of iPSCs, we performed detailed characterization of iPSC lines established w/wo transient p53 suppression. All iPSC lines were highly similar with respect to expression of pluripotency markers and showed a comparable upregulation of TP53 and downregulation of P21 compared to NHDFs. Methylation analyses showed a comparable hypomethylation of the pluripotency-associated genes OCT4, NANOG, SALL4, and RAB25 and hypermethylation of the fibroblast-specific gene UBE1L, as previously reported for iPSCs and ESCs (Nishino et al., 2011). Furthermore, genome-wide transcriptome analyses showed no significant up- or downregulated genes and analysis with PluriTest, which is a fast and ethically superior alternative to teratoma assays in mice (Buta et al., 2013), showed that all the iPSC lines clustered within the predefined pluripotency and novelty scores. Finally, in vitro

Figure 3. iPSCs Generated by Transient p53 Suppression Display Normal In Vitro Characteristics

(A–H) (A and E) Phase contrast morphology and (B–H) immunocytochemical staining of induced pluripotent stem cells (iPSCs) generated with or without (w/wo) a short hairpin to p53 (shp53) with the pluripotency markers OCT3/4, TRA1-81, and Hoechst (B and F), NANOG, TRA1-60, and Hoechst (C and G), and SSEA3, SSEA4, and Hoechst (D and H).

(I) Quantitative real-time PCR with the pluripotency markers ZFP42, POU5F1 (OCT4), SOX2, NANOG, DNMT3B, and TP53 and P21. Relative expression is shown as the fold change ($2^{-\Delta\Delta Ct}$) with normal human dermal fibroblasts (NHDFs) as reference. A commercial iPSC line (SBI) was included.

(J) Schematic view of the methylation state of selected CpG sites in POU5F1 (OCT4), SAL4, RAB25, and UBE1L. Each row represents a separate clone and each circle represents a CpG site. Open circles represent unmethylated sites and black circles represent methylated sites.

(K) PluriTest algorithm results of transcriptome profiles including a reference iPSC line (SBI) and NHDFs. The PluriTest results are plotted in a density distribution for previously referenced pluripotent stem cells (red cloud) and somatic cells (blue cloud).
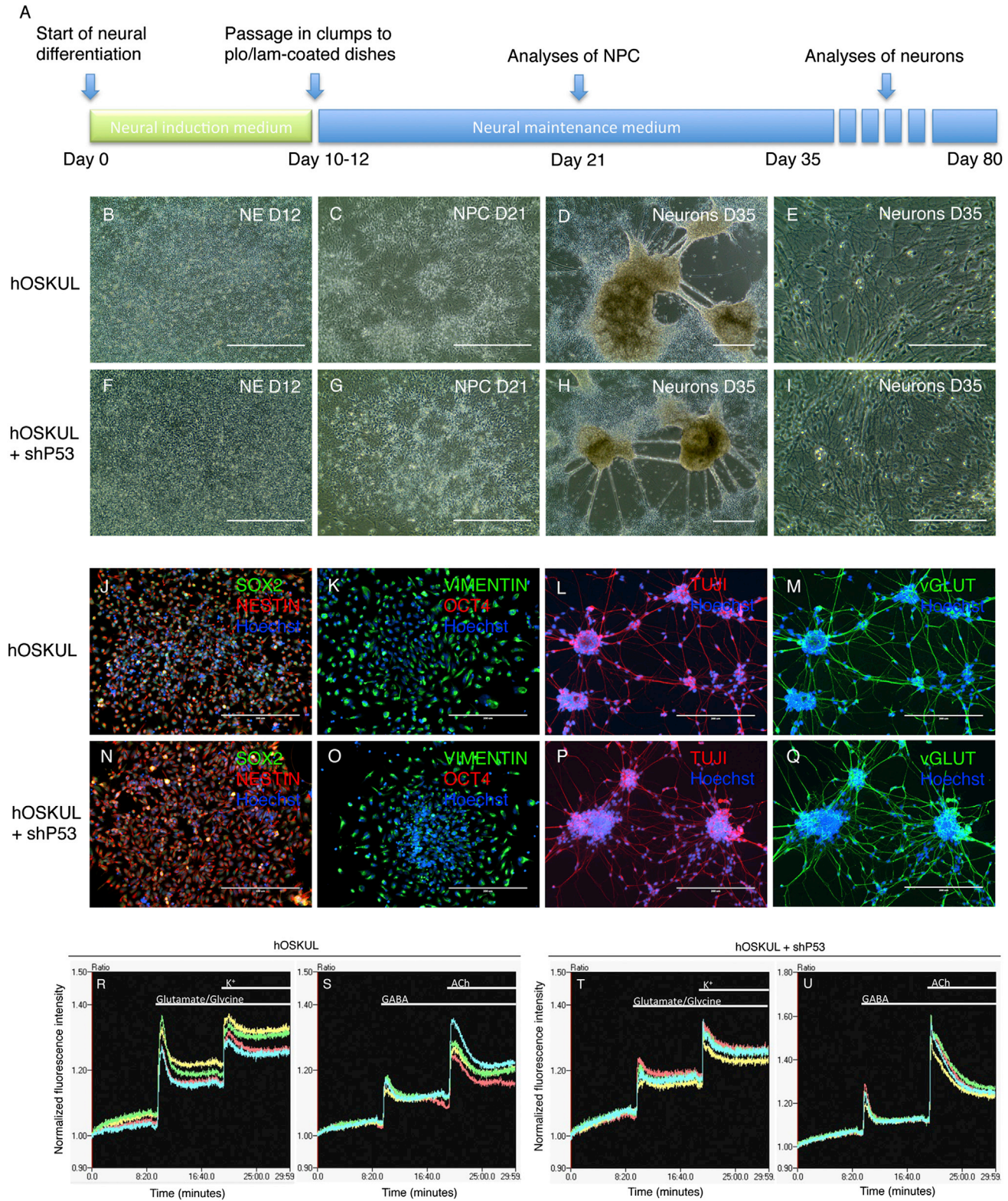
(L–S) (L, M, P, and Q) Morphology of embryoid bodies (EBs) on day 7 (L and P), plated EBs on day 28 (M and Q), and immunocytochemical staining of plated EBs on day 28 with TUJI (N and R), smooth muscle actin (SMA), and alpha-fetoprotein (AFP) (O and S).

Scale bars, 400 μm (A, E, L, M, P, and Q), 100 μm (B–D and F–H), or 200 μm (N, O, R, and S). See also Figure S3 and Tables S1–S3.

Figure 4. iPSCs Generated by Transient p53 Suppression Can Differentiate to Functional Neurons In Vitro

(A) Timeline showing the directed neural differentiation of induced pluripotent stem cell (iPSC) lines generated with or without (w/wo) a short hairpin to p53 (shp53).

(legend continued on next page)

differentiation confirmed the potential of the iPSC lines to generate cells of the three germ layers. To date, some of the iPSC lines (K1 and K1_shp53) have been cultured for more than 35 passages, without showing signs of reduced proliferation.

iPSCs present an ideal system for studies on genomic stability and confer the ability to determine whether a given alteration is new, because the parental cells can also be analyzed (Laurent et al., 2011). The iPSC lines generated w/wo shp53 displayed normal karyotypes, and structural CNV analyses showed that they contained between zero and five CNVs (1.66 CNVs in average), which were not present in the parental NHDFs. These numbers are comparable with recent reports using single-nucleotide variants (SNVs) analyses that reported an average of five coding mutations, of which around half was preexisting in the parental fibroblasts (Cheng et al., 2012; Gore et al., 2011). Moreover, no significant difference between the overall numbers of CNVs in iPSC lines generated w/wo transient p53 suppression was found, thus corroborating recent studies that demonstrated that episomal reprogramming is not inherently mutagenic (Cheng et al., 2012; Gore et al., 2011).

Lin and colleagues reported that *tp53* knockout ESC showed impaired differentiation and remained in a pluripotent state (Lin et al., 2005). In contrast, transient p53 suppression did not affect the neural differentiation potential, and all the iPSC lines successfully formed NPCs and functional neurons. Recently, transplantation of NPCs from plasmid-derived iPSCs (Yu et al., 2009) was reported to increase the neurovascular coupling and behavioral recovery in a mouse model of ischemic stroke without any signs of tumor formation 1 year after transplantation (Mohamad et al., 2013). In accordance, transplantation of NPCs from the iPSC lines established by transient p53 suppression in relevant animal models would be highly useful for evaluation of safety and efficacy in regenerative stem cell therapy.

The present study demonstrates that transient p53 suppression increases reprogramming efficiency without affecting apoptosis and DNA damage. Furthermore, iPSC lines generated w/wo transient p53 suppression are identical with respect to their pluripotent phenotype, their mutational load, and their differentiation capacity, rendering the method suitable for in vitro studies on patient-specific disease pathology with a potential for clinical translation.

EXPERIMENTAL PROCEDURES

A complete description of experimental procedures can be found in Supplemental Experimental Procedures.

Reprogramming
Normal human dermal fibroblasts (NHDFs; Lonza) were electroporated with plasmids encoding *hOCT4* or *hOCT4* with a short hairpin to *TP53* (shp53) in combination with *hSOX2*, *hKLF4*, *hL-MYC*, and *hLIN28* (Addgene plasmids 27076, 27077, 27078 and 27080), abbreviated hOSKUL or hOSKUL + shp53, respectively (Okita et al., 2011, 2013) and cultured in mTeSR1 medium (STEMCELL Technologies) and Matrigel-coated dishes (BD Biosciences) from day 7 to day 28.

Flow Cytometry and Apoptotic Measurements
Flow cytometry was performed with monoclonal antibodies against SSEA4 and TRA1-60 (BD Biosciences), p53, p21, H2A.X (Cell Signaling Technology), and PUMA (Novus Biologicals) on a FACSarray Bioanalyzer or a BD Accuri C6 (BD Biosciences). Unlabeled and isotype-labeled NHDFs were used as controls for gating.

Characterization of iPSC Lines
Six iPSC lines were established with hOSKUL (K1, K2, and K3) or hOSKUL + shp53 (K1_shp53, K2_shp53, and K3_shp53) and characterized at passage 10 according to established pluripotency criteria (Martí et al., 2013). Genome-wide transcriptome analysis was performed using the HT12 v4 BeadChip microarray (Illumina). DNA methylation analyses were performed with the Cells-to-CpG Bisulfite Conversion Kit (Life Technologies), and PCR-amplified sequences from ten clones per chromosomal region were examined. Primers are specified in Table S2.

Chromosome Studies and Copy Number Variation Analyses
Metaphase chromosomes were investigated with G-banding using standard procedures. Copy number variation (CNV) analysis was performed using the high resolution CytoScan HD chromosome microarray platform (Affymetrix), and data were processed using Affymetrix Chromosome Analysis Suite (ChAS) and manually corrected for false-positive hits.

(B–I) Phase contrast morphology of neuroepithelium (NE) at day 12 (B and F), neural progenitor cells (NPC) at day 21 (C and G), and neurons at day 35 (D, E, H, and I).

(J–Q) Immunocytochemistry of NPCs at day 21 with SOX2, NESTIN, and Hoechst (J and N) and VIMENTIN, OCT4, and Hoechst (K and O) and of neurons at day 35 with TUJI and Hoechst (L–P) and vGLUT and Hoechst (M and Q).

(R–U) Intracellular calcium kinetics in iPSC-derived neurons generated without (R and S) or with shp53 (T and U). Baseline fluorescence was recorded for 10 min before application of 300 μM glutamate/10 μM glycine, 25 mM K$^+$, 100 μM GABA and 300 μM acetylcholine. The fluorescence was normalized to the first data point of each of the traces.

Scale bars, 200 μm (B–D, F–H, and J–Q) and 100 μm (E and I).

Stem Cell Reports

Effects of Transient p53 Suppression on Human iPSCs

Directed Neural Differentiation

Directed neural differentiation was carried out according to Shi et al. (2012). Primary antibodies are listed in Table S3.

Statistical Analyses

Statistical analyses comprised a two-tailed Student's t test with *$p < 0.05$ considered significant.

ACCESSION NUMBERS

The GEO (http://www.ncbi.nlm.nih.gov/geo/) accession number for the microarray data reported in this paper is GSE48665. CNV raw data are available upon request.

SUPPLEMENTAL INFORMATION

Supplemental Information includes Supplemental Experimental Procedures, three figures, and three tables and can be found with this article online at http://dx.doi.org/10.1016/j.stemcr.2014.07.006.

REFERENCES

Brosh, R., Assia-Alroy, Y., Molchadsky, A., Bornstein, C., Dekel, E., Madar, S., Shetzer, Y., Rivlin, N., Goldfinger, N., Sarig, R., and Rotter, V. (2013). p53 counteracts reprogramming by inhibiting mesenchymal-to-epithelial transition. Cell Death Differ. 20, 312–320.

Buta, C., David, R., Dressel, R., Emgård, M., Fuchs, C., Gross, U., Healy, L., Hescheler, J., Kolar, R., Martin, U., et al. (2013). Reconsidering pluripotency tests: do we still need teratoma assays? Stem Cell Res. (Amst.) 11, 552–562.

Campbell, K.H., McWhir, J., Ritchie, W.A., and Wilmut, I. (1996). Sheep cloned by nuclear transfer from a cultured cell line. Nature 380, 64–66.

Chen, Z., Zhao, T., and Xu, Y. (2012). The genomic stability of induced pluripotent stem cells. Protein and cell 3, 271–277.

Cheng, L., Hansen, N.F., Zhao, L., Du, Y., Zou, C., Donovan, F.X., Chou, B.-K., Zhou, G., Li, S., Dowey, S.N., et al.; NISC Comparative Sequencing Program (2012). Low incidence of DNA sequence

variation in human induced pluripotent stem cells generated by nonintegrating plasmid expression. Cell Stem Cell 10, 337–344.

Dolezalova, D., Mraz, M., Barta, T., Plevova, K., Vinarsky, V., Holubcova, Z., Jaros, J., Dvorak, P., Pospisilova, S., and Hampl, A. (2012). MicroRNAs regulate p21(Waf1/Cip1) protein expression and the DNA damage response in human embryonic stem cells. Stem Cells 30, 1362–1372.

Fusaki, N., Ban, H., Nishiyama, A., Saeki, K., and Hasegawa, M. (2009). Efficient induction of transgene-free human pluripotent stem cells using a vector based on Sendai virus, an RNA virus that does not integrate into the host genome. Proc. Jpn. Acad., Ser. B, Phys. Biol. Sci. 85, 348–362.

Garcia-Canton, C., Anadón, A., and Meredith, C. (2012). γH2AX as a novel endpoint to detect DNA damage: applications for the assessment of the in vitro genotoxicity of cigarette smoke. Toxicol. In Vitro 26, 1075–1086.

Godar, S., Ince, T.A., Bell, G.W., Feldser, D., Donaher, J.L., Bergh, J., Liu, A., Miu, K., Watnick, R.S., Reinhardt, F., et al. (2008). Growth-inhibitory and tumor-suppressive functions of p53 depend on its repression of CD44 expression. Cell 134, 62–73.

Gore, A., Li, Z., Fung, H.-L., Young, J.E., Agarwal, S., Antosiewicz-Bourget, J., Canto, I., Giorgetti, A., Israel, M.A., Kiskinis, E., et al. (2011). Somatic coding mutations in human induced pluripotent stem cells. Nature 471, 63–67.

Hong, H., Takahashi, K., Ichisaka, T., Aoi, T., Kanagawa, O., Nakagawa, M., Okita, K., and Yamanaka, S. (2009). Suppression of induced pluripotent stem cell generation by the p53-p21 pathway. Nature 460, 1132–1135.

Kahler, D.J., Ahmad, F.S., Ritz, A., Hua, H., Moroziewicz, D.N., Sproul, A.A., Dusenberry, C.R., Shang, L., Paull, D., Zimmer, M., et al. (2013). Improved methods for reprogramming human dermal fibroblasts using fluorescence activated cell sorting. PLoS ONE 8, e59867.

Kawamura, T., Suzuki, J., Wang, Y.V., Menendez, S., Morera, L.B., Raya, A., Wahl, G.M., and Izpisúa Belmonte, J.C. (2009). Linking the p53 tumour suppressor pathway to somatic cell reprogramming. Nature 460, 1140–1144.

Lake, B.B., Fink, J., Klemetsaune, L., Fu, X., Jeffers, J.R., Zambetti, G.P., and Xu, Y. (2012). Context-dependent enhancement of induced pluripotent stem cell reprogramming by silencing Puma. Stem Cells 30, 888–897.

Laurent, L.C., Ulitsky, I., Slavin, I., Tran, H., Schork, A., Morey, R., Lynch, C., Harness, J.V., Lee, S., Barrero, M.J., et al. (2011). Dynamic changes in the copy number of pluripotency and cell proliferation genes in human ESCs and iPSCs during reprogramming and time in culture. Cell Stem Cell 8, 106–118.

Lin, T., Chao, C., Saito, S., Mazur, S.J., Murphy, M.E., Appella, E., and Xu, Y. (2005). p53 induces differentiation of mouse embryonic stem cells by suppressing Nanog expression. Nat. Cell Biol. 7, 165–171.

Marión, R.M., Strati, K., Li, H., Murga, M., Blanco, R., Ortega, S., Fernandez-Capetillo, O., Serrano, M., and Blasco, M.A. (2009). A p53-mediated DNA damage response limits reprogramming to ensure iPS cell genomic integrity. Nature 460, 1149–1153.

Martí, M., Mulero, L., Pardo, C., Morera, C., Carrió, M., Laricchia-Robbio, L., Esteban, C.R., and Izpisua Belmonte, J.C. (2013). Characterization of pluripotent stem cells. Nat. Protoc. 8, 223–253.

Martins-Taylor, K., and Xu, R.-H. (2012). Concise review: Genomic stability of human induced pluripotent stem cells. Stem Cells 30, 22–27.

Menendez, S., Camus, S., and Izpisua Belmonte, J.C. (2010). p53: guardian of reprogramming. Cell Cycle 9, 3887–3891.

Mohamad, O., Drury-Stewart, D., Song, M., Faulkner, B., Chen, D., Yu, S.P., and Wei, L. (2013). Vector-free and transgene-free human iPS cells differentiate into functional neurons and enhance functional recovery after ischemic stroke in mice. PLoS ONE 8, e64160.

Ng, S., Bazett-Jones, D.P., Alitalo, K., Lahesmaa, R., Nagy, A., and Otonkoski, T. (2011). Copy number variation and selection during reprogramming to pluripotency. Nature 471, 58–62.

Nishino, K., Toyoda, M., Yamazaki-Inoue, M., Fukawatase, Y., Chikazawa, E., Sakaguchi, H., Akutsu, H., and Umezawa, A. (2011). DNA methylation dynamics in human induced pluripotent stem cells over time. PLoS Genet. 7, e1002085.

Okita, K., Matsumura, Y., Sato, Y., Okada, A., Morizane, A., Okamoto, S., Hong, H., Nakagawa, M., Tanabe, K., Tezuka, K., et al. (2011). A more efficient method to generate integration-free human iPS cells. Nat. Methods 8, 409–412.

Okita, K., Yamakawa, T., Matsumura, Y., Sato, Y., Amano, N., Watanabe, A., Goshima, N., and Yamanaka, S. (2013). An efficient nonviral method to generate integration-free human-induced pluripotent stem cells from cord blood and peripheral blood cells. Stem Cells 31, 458–466.

Shi, Y., Kirwan, P., and Livesey, F.J. (2012). Directed differentiation of human pluripotent stem cells to cerebral cortex neurons and neural networks. Nat. Protoc. 7, 1836–1846.

Takahashi, K., and Yamanaka, S. (2006). Induction of pluripotent stem cells from mouse embryonic and adult fibroblast cultures by defined factors. Cell 126, 663–676.

Yu, J., Hu, K., Smuga-Otto, K., Tian, S., Stewart, R., Slukvin, I.I., and Thomson, J.A. (2009). Human induced pluripotent stem cells free of vector and transgene sequences. Science 324, 797–801.

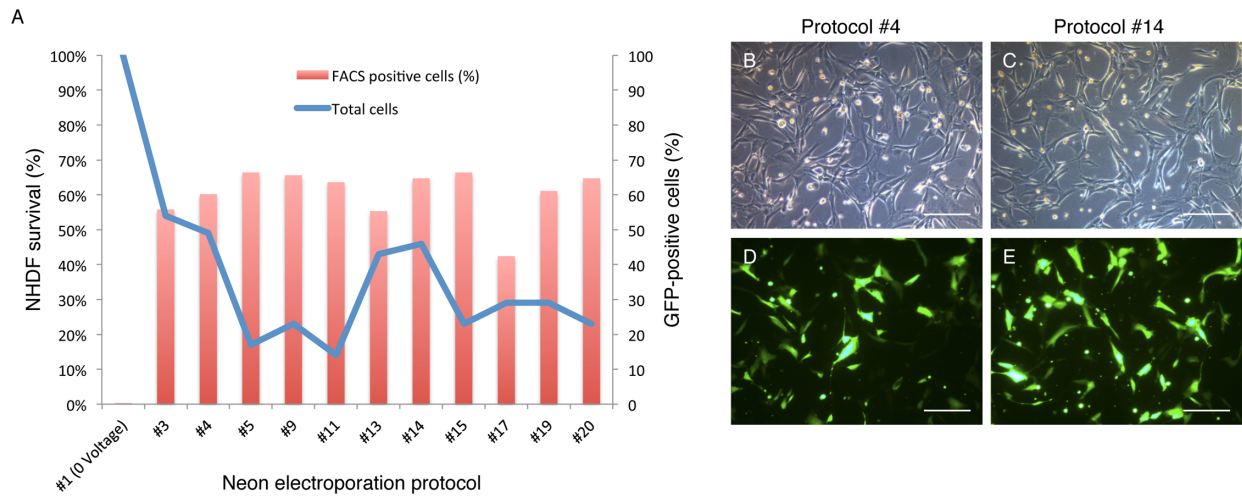# Transient p53 Suppression Increases Reprogramming of Human Fibroblasts without Affecting Apoptosis and DNA Damage

Mikkel A. Rasmussen, Bjørn Holst, Zeynep Tümer, Mads G. Johnsen, Shuling Zhou, Tina C. Stummann, Poul Hyttel, and Christian Clausen

Figures

Figure S1. Optimization of non-integrative reprogramming procedure, related to Figure 1. A) Survival and flow cytometry analyses of normal human dermal fibroblasts (NHDFs) one day after electroporation with a GFP plasmid using a Neon^{TM} electroporation device at different conditions. B-E). Phase contrast morphology and green fluorescent protein (GFP) fluorescence of NHDFs electroporated with a single pulse at 1600 V for 20 ms (Protocol #4; B, D) or two pulses at 1200 V for 20 ms (Protocol #14; C, E). Scale bars correspond to 200 μm.
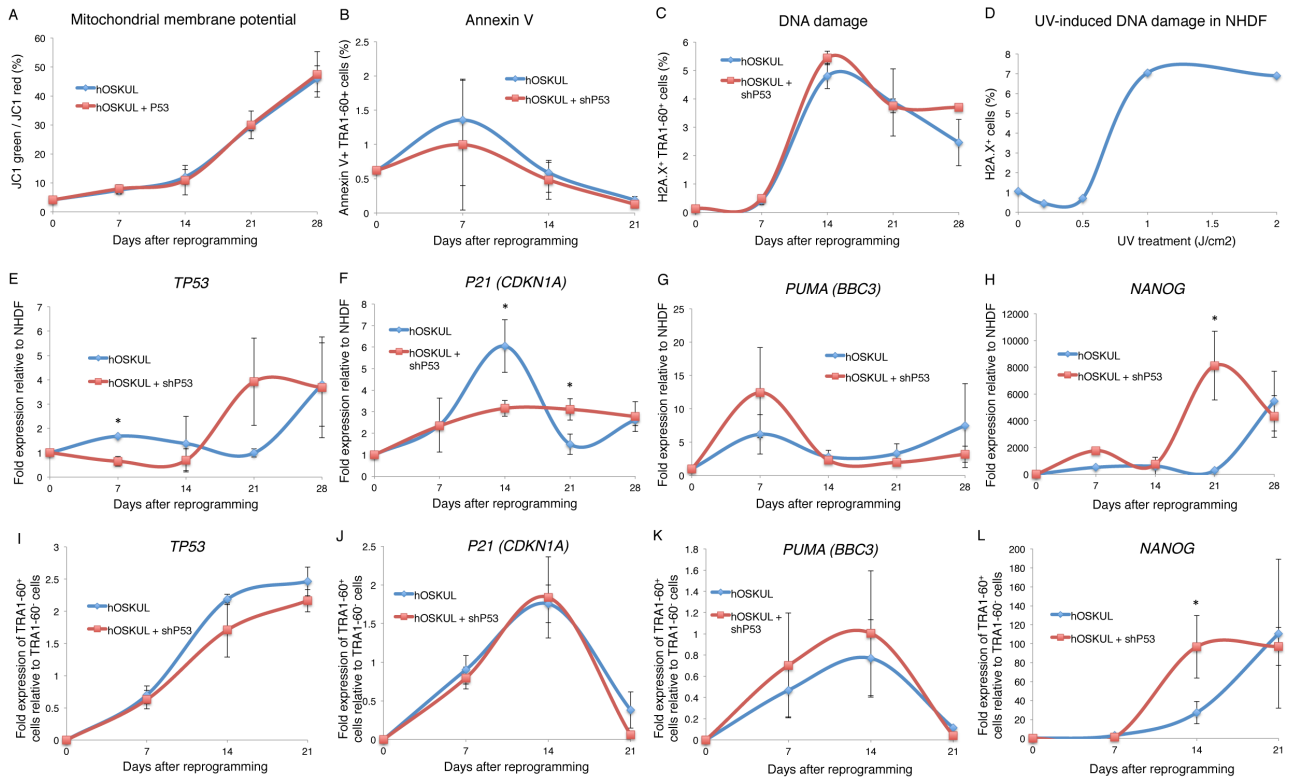
Figure S2. Apoptosis, DNA damage and expression of *P53*, *P21*, *PUMA* and *NANOG* during reprogramming with or without (w/wo) a short hairpin to p53 (shp53), related to Figure 2. Normal human dermal fibroblasts (NHDFs) were analyzed on day 0, 7, 14, 21 (and 28) after reprogramming with the episomal plasmids *hOCT4*, *hSOX2*, *hKLF4*, *hL-MYC* and *hLIN28* (hOSKUL) w/wo shp53. A) Mitochondrial membrane potential assay with the dyes JC-1 and DAPI. In apoptotic cells, the mitochondrial potential collapses and the monomeric form of JC-1 shows green fluorescence. B) Flow cytometry of cells double positive for Annexin V and TRA1-60. C) Flow cytometry of cells double positive for the DNA damage marker H2A.X and TRA 1-60. D) Flow cytometry with H2A.X of NHDFs subjected to different doses of ultraviolet radiation. E-L) Quantitative real-time PCR analyses in the total cell population (E-H) or in TRA1-60 sorted cells (I-L) after reprogramming w/wo shP53. E, I) *TP53*, F, J) *P21,* G, K) *PUMA* and H, L) *NANOG*. Relative expression is shown as the fold change ($2^{-\Delta\Delta Ct}$) with NHDFs as reference and GAPDH as reference gene. Y error bars depict standard deviation of three independent experiments. *p<0.05.

A
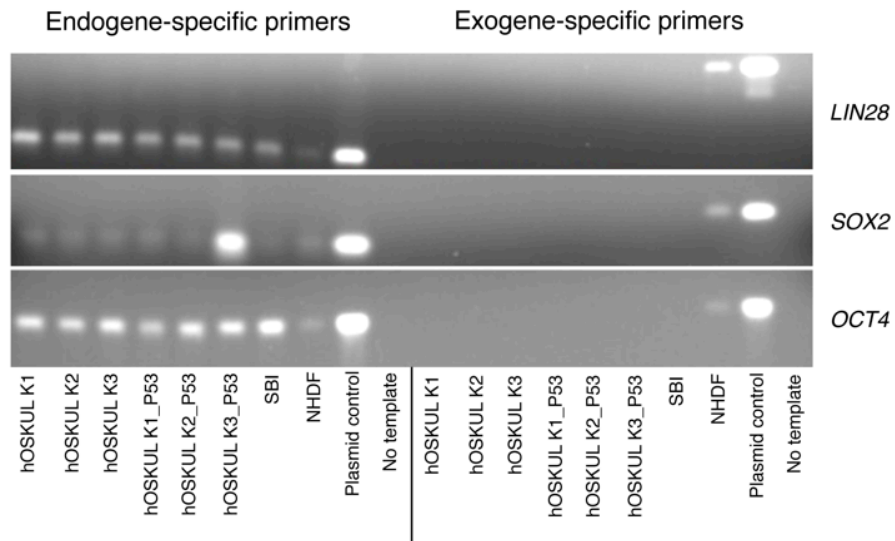
B
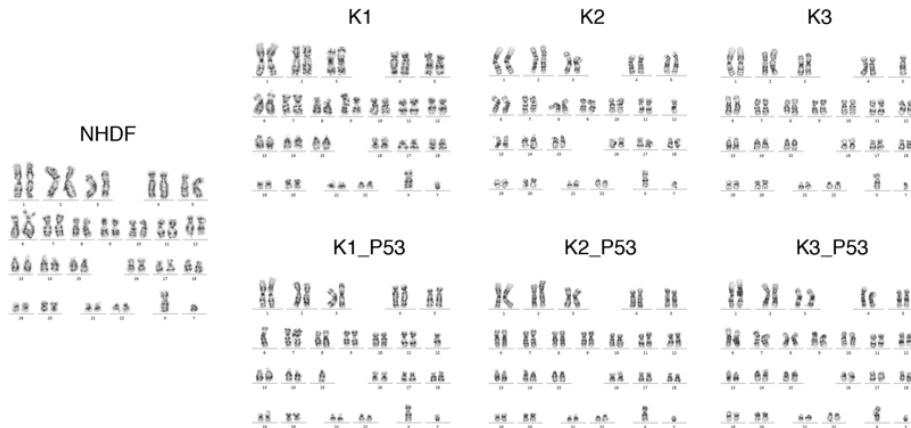
Figure S3. Expression analysis of episomal vectors in iPSC lines and karyotyping of induced pluripotent stem cell lines, related to Figure 3. A) Reverse-transcriptase PCR at passage 10 with the endogenous and exogenous pluripotency genes *LIN28*, *SOX2,* and *OCT4* in iPSC lines generated with or without a short hairpin to p53. Normal human dermal fibroblasts (NHDFs) transfected two days before with hOSKUL served as a positive control and a sample without template served as negative control. An iPSC line (SBI) generated by lentivirus was included as a reference. B) Representative karyotypes of the founder normal human dermal fibroblasts (NHDFs) and induced pluripotent stem cell (iPSC) lines generated with or without a short hairpin to p53 (shp53).

Tables

Table S1. Copy number variations in induced pluripotent stem cell lines, related to Figure 3.

iPSC line[1]	Type	Chr[2]	Band	Start position	End position	Size (kb)[3]	Genes within the CNV[4]	DGV[5]
K1	Gain	1	q44	245500158	245787005	287	*KIF26B*	Variation
K1	Gain	3	p12.2	81531958	82762047	1230	*GBE1*	Variation
K3	Loss	2	q33.3	205758866	205984167	225	*PARD3B*	Variation
K1_shp53	Gain	5	q34	167784954	167951642	167	*WWC1, RARS*	
K1_shp53	Loss	7	q11.22	69672679	70023881	351	*AUTS2*	
K1_shp53	Loss	7	q31.1	110709365	110842032	133	*IMMP2L, LRRN3*	Variation
K1_shp53	Gain	10	q21.1	53966718	54049359	83	*PRKG1*	Variation
K1_shp53	Loss	12	q23.1	100658499	100697244	39	*DEPDC4, SCYL2*	Variation
K2_shp53	Loss	13	q31.3	94337996	94506524	169	*GPC6*	Variation
K3_shp53	Loss	X	q21.33	94049304	94129700	80		

[1]Induced pluripotent stem cell line, [2]chromosome, [3]kilobases, [4]copy number variation, [5]database of genomic variance.

Table S2. Primers used for methylation analyses, related to Figure 3.

Gene relation	Primer names	Primer sequences[1] 5'-3'	Product sizes (bp)	Products chromosomal extend[2]
NANOG	ConNRR-F1	ttATATTttTGATTTAAAAGTTGGAAA	298	Chromosome 12
	ConNRR-R1	aaCAACCAaCTCAaTCCAaCAaAAC		701.877 -702.174
POU5F1	ConOCT4-3-F	AttTGttTTTTGGGtAGTTAAAGGt	221	Chromosome 6
(OCT4)	ConOCT4-3-R	CCAaCTaTCTTCATCTTaaTaaCATCC		31.080.784-31.080.564
RAB25	ConRAB25-F1	AGGGGtTATTTtTTGtTtATTAGTTG	178	Chromosome 1
	ConRAB25-R1	TaaaTaTCTaCTCTCAaCCTaaaCTCCC		7.519.337-7.519.514
SALL4	ConSALL4-F1	GGttAATtAGtTGTtAGGGtTtATGA	110	Chromosome 20
	ConSALL4-R2	TCCTaaAaTTaaaAAATTTACCCCC		20.615.097-20.615.206
UBE1L	ConUBE1L-F1	GtTTGGttTTGGTTttTGTTTGtAt	169	Chromosome 3

ConUBE1L-R1   aAATACAaCTCCTCATCCAaTAaCTTC   49.791.174-49.791.342

[1]Lower case 't' corresponds to a cytosine in the unconverted target sequence. Lower case 'a' corresponds to a guanine in the unconverted target sequence. [2]Genome Reference Consortium Human Build 37.

Table S3. Antibodies used for confirmation of pluripotency and *in vitro* differentiation, related to Figure 3 and 4.

	Antibody and host species	Dilution	Company and catalog number
Pluripotency	rabbit anti-NANOG	1:500	Peprotech, 500-P236
	goat anti-OCT4	1:500	Santa Cruz, sc-8628
	rat anti-SSEA3	1:100	Biolegend, 330302
	mouse anti-SSEA4	1:100	Biolegend, 330402
	mouse anti-Tra-1-81	1:200	Biolegend, 330702
	mouse anti-Tra-1-60	1:200	Biolegend, 330602
In vitro	mouse anti-Smooth muscle actin (SMA)	1:500	DAKO, M0851
differentiation	rabbit anti-Alpha-1-fetoprotein (AFP)	1:500	DAKO, A0008
	mouse anti-Beta-III-tubulin (TUJI)	1:4000	Sigma-Aldrich, T8660
	mouse anti-SOX2	1:100	RD systems, MAB2018
	rabbit anti-NESTIN	1:4000	Millipore, ABD69
	mouse anti-VIMENTIN	1:500	DAKO M0725
	sheep anti-VGLUT1	1:200	Abcam, AB79774

Supplemental Experimental Procedures

Unless otherwise stated, consumables and reagents were purchased from Sigma-Aldrich, St. Louis, MO, USA. Plasmids were purchased from Addgene, Cambridge, MA, USA.

Reprogramming of normal human dermal fibroblasts and establishment of iPSC lines

NHDFs (Lonza, CC-2511) from an 18-year-old male (XY NHDF) and a 32-year-old female (XX NHDF) were cultured in fibroblast medium consisting of Dulbecco's Modified Eagle Medium (DMEM) supplemented with 10% fetal bovine serum (FBS), 2 mM L-glutamine, penicillin and streptomycin (Pen/Strep) and 2 ng/ml basic fibroblast growth factor (bFGF; Miltenyi Biotech, Bergisch Gladbach, Germany).

At passage 5-6, the NHDFs from a 18-year old healthy male were trypsinized and 10^5 cells were electroporated with a total of 1µg of the episomal plasmids *hOCT4* (Addgene plasmid #27076) or *hOCT4* with a short hairpin to *TP53* (shp53; Addgene plasmid #27077) in combination with *hSOX2* and *hKLF4*, (Addgene plasmid #27078) and *hL-MYC* and *hLIN28* (Addgene plasmid #27080), abbreviated *hOSKUL* or *hOSKUL* + shp53*, respectively. As a control, a fibroblast line from the same NHDF line was electroporated with a PLK.O-shp53 plasmid (Godar et al., 2008) and stable clones expressing shp53 were selected using puromycin. The electroporation was performed using a Neon™ electroporation device (Life Technologies, Carlsbad, CA, USA) with a single pulse at 1600 V for 20 ms or two pulses at 1200 V for 20 ms. Optimization of the electroporation procedure was performed with an episomal GFP plasmid (Addgene plasmid #27082).

Immediately after electroporation, the cells were transferred to a single well of a 6-well culture dish containing warm fibroblast medium without Pen/Strep, which was changed the day after to fibroblast medium with Pen/Strep. Seven days after electroporation, NHDFs were trypsinized and split 1:2 onto hESC-qualified Matrigel-coated dishes (BD Biosciences, Franklin

Lakes, NJ, USA) and cultured in mTeSR1 medium (Stem Cell Technologies, Vancouver, BC, Canada) in 5% O_2, 5% CO_2 in N_2 with the medium replenished every other day.

On day 28, six iPSC lines were established from the same XY NHDF donor using the plasmids *hOSKUL* (named K1, K2 and K3) or *hOSKUL* + shp53 (named K1_shp53, K2_shp53 and K3_shp53). The primary iPSC colonies were dissected out manually by needles and transferred to new Matrigel-coated 6-well dishes and cultured in mTeSR1. After a second manual passage, the iPSC lines were split 1:6 every 5-6 days with Dispase (Stem Cell Technologies, Vancouver, BC, Canada). At passage 10, the iPSC lines were harvested for subsequent analyses or frozen in CryoStem freezing medium (Stemgent, Cambridge, MA, USA).

Alkaline Phosphatase and TRA1-81 live staining

On day 28 after reprogramming, iPSC colonies were live stained for 30 min with a TRA1-81 antibody (Stemgent, Cambridge, MA, USA) or fixed in 4% paraformaldehyde (PFA) and stained for Alkaline phosphatase (AP) using an AP detection kit (Merck-Millipore, Billerica, MA, USA). The total numbers of AP-positive iPSC colonies were quantified using a stereomicroscope.

Flow cytometry

On day 0 (NHDFs) and on days 7, 14, 21 and 28 after reprogramming, cells were trypsinized and washed in flow buffer containing 1% bovine serum albumin (BSA) in Dulbecco's Phosphate-Buffered Saline (DPBS). Cells were either incubated for 45 min with a combination of APC conjugated anti-SSEA4 (BD Biosciences, Franklin Lakes, NJ, USA) and PE conjugated anti-TRA-1-60 (BD Biosciences, Franklin Lakes, NJ, USA or fixed for 15 min with 4% PFA, incubated for 30 min in 90% ice-cold methanol and incubated with Alexaflour 488-conjugated anti-p53, anti-p21, anti-phospho-histone H2A.X (Ser139) antibody (Cell Signaling Technology, Danvers, MA, USA)

or DyLight 488-conjugated anti-PUMA (Novus Biologicals, Littleton, USA) and PE-conjugated anti-SSEA4 and 647-conjugated anti-TRA-1-60 (BD Biosciences, Franklin Lakes, NJ, USA). After washing twice in flow buffer, flow cytometric analysis was performed with a BD FACSarray Bioanalyzer or a BD Accuri C6 (BD Biosciences, Franklin Lakes, NJ, USA). Unlabeled and isotype labeled NHDF's were used as controls for gating. As a positive control, NHDFs were exposed to different ultraviolet (UV) treatments at 254 nm, ranging from 0, 0.2, 0.5, 1 and 2 J/cm^2.

Apoptotic measurements

Apoptosis was measured by a mitochondrial membrane potential assay (Chemometec, Alleroed, Denmark). Briefly, cells were stained with the dyes JC-1 and DAPI. In healthy cells, JC-1 forms aggregates showing red fluorescence, whereas, in apoptotic cells the mitochondrial potential collapses and JC-1 localizes to the cytosol in its monomeric form showing green fluorescence. Quantification of green and red JC-1 fluorescence was carried out by use of a Nucleocounter NC-3000 (Chemometec Alleroed, Denmark).

Immunofluorescence staining

At passage 10, all iPSC lines were fixed with 4% PFA in PBS for 15 min and stained by standard immunofluorescence staining procedures. The primary antibodies (Supplementary table 1) were visualized with the secondary antibodies Alexa 488 or Alexa 594 diluted 1:400 (Life technologies, Carlsbad, CA, USA) and counterstained with Hoechst bisbenzimide 33258. Images were acquired on a Leica DMRB-fluorescence microscope (Leica Microsystems, Wetzlar, Germany).

Quantitative real-time polymerase chain reaction (qRT-PCR)

Total RNA was purified from unsorted and TRA1-60 sorted cells during reprogramming as well as

from six iPSC lines at passage 10 and NHDFs by RNeasy kit (Qiagen, Hilden, Germany).

Conversion to cDNA and quantitative real-time PCR (qRT-PCR) were performed using TaqMan

RNA-to-C$_T$^{TM} 1-step kit (Life Technologies, Carlsbad, CA, USA). Primers for qRT-PCR (Life

Technologies, Carlsbad, CA, USA) included *SOX2*, *ZFP42*, *NANOG*, *POU5F1 (OCT4)*, *DNMT3B*,

TP53, *P21* (*CDKN1A*), *PUMA* (*BBC3*) and *GAPDH*. Relative quantification was calculated using $2^{-\Delta\Delta Ct}$ with NHDFs as a reference and GAPDH as reference gene. A commercial iPSC line (named

SBI; System Biosciences, Mountain view, CA, USA), generated by viral transduction of human

foreskin fibroblasts with *OCT4*, *SOX2*, *KLF4* and *C-MYC*, was used as a positive control.

In vitro **differentiation**

Embryoid body (EB) formation was performed by transferring Dispase-treated clumps of iPSC to

ultra-low attachment plates (Corning, Corning, NY, USA) in mTeSR1. After 2 days of culturing,

the medium was changed to DMEM/F12 containing 20% knockout serum replacement (Life

Technologies, Carlsbad, CA, USA), 1x non-essential amino acid, 2 mM L-glutamine, 0.1 mM 2-

mercaptoethanol and 1% pen/strep. After 7 days, the EBs were plated on 0.1% gelatin-coated

culture dishes and cultured in DMEM supplemented with 10% FBS, 2 mM L-gultamine and 1%

pen/strep for up to three weeks. The cells were fixed for 15 min in 4% PFA for

immunocytochemical analyses with antibodies of TUJI, SMA and AFP (Supplementary table 1).

Karyotyping

At passage 10, all iPSC lines and NHDFs were treated for 45 min with KaryoMAX colcemid (Life

Technologies, Carlsbad, CA, USA) and harvested in fresh fixative containing 25% acetic acid and

75% methanol. Karyotyping was performed on G-banded metaphase chromosomes using standard

procedures. At least 10 metaphases were analyzed per sample with an approximate resolution of 550 to 600 bands per haploid genome.

Genome wide transcriptome analysis

For whole transcriptome microarray analysis, RNA was isolated from the iPSC lines K1 and K1_shp53 at passage 16, K2 and K2_shp53 at passage 12 and K3 and K3_shp53 at passage 13, as well as NHDFs and SBI iPSC with RNeasy Kit (Qiagen, Hilden, Germany). cDNA was hybridized to a HT12 v4 BeadChip microarray (Illumina, San Diego, CA, USA), which contains more than 47.000 probes for known human genes. Raw data were analyzed with the PluriTest algorithm (www.pluritest.org) or processed in Genome Studio data analysis software (Illumina, San Diego, CA, USA) using quantile normalization and a detection p-value of < 0.01 and subsequently analyzed in Multi Experiment Viewer (www.tm4.org) using a comparative t-test with Bonferroni correction and $p < 0.05$.

Copy number variation (CNV) analyses

DNA was purified from all iPSC lines at passage 10 and founder NHDFs using Wizard genomic DNA purification kit (Promega, Madison, WI, USA). CNV analysis was performed using the high resolution CytoScan HD chromosome microarray platform (Affymetrix, Santa Clara, CA, USA), which provides 750.000 polymorphic (SNP, single nucleotide polymorphism) and 1.900.000 non-polymorphic (CNV) markers. Raw data were processed using Affymetrix Chromosome Analysis Suite (ChAS) and manually corrected for false positive hits. To prevent false positive CNVs arising due to inherent microarray "noise", gains and losses of > 30kb (and >30 consecutive probes) were taken into consideration (confidence limit $> 90\%$). The identified CNVs were compared with the Database of Genomic Variants (DGV; http://projects.tcag.ca/variation/) and 1038 phenotypically

healthy samples run on the same platform to exclude common variants. The data were interpreted using the UCSC Genome Browser (http://genome.ucsc.edu). Data is available upon request.

Directed neural differentiation

Directed neural differentiation was carried out according to Shi and colleagues (Shi et al., 2012), with minor modifications. Briefly, iPSC lines generated w/wo shp53 (n=6) were cultured in mTeSR1 and ESC-qualified Matrigel until they reached 70-80% confluence. The medium was then changed to neural induction medium (NIM) consisting of DMEM/F12 and Neurobasal medium (1:1; Life Technologies, Carlsbad, CA, USA), 1 x N2 and 1 x B-27 minus Vitamin A (both from Life Technologies Carlsbad, CA, USA), 1mM Glutamax and Pen/Strep including the dual SMAD inhibitors LDN193189 (0.2 μM) and SB431542 (10 μM). After 10-12 days, the cells were split 1:3 with Dispase onto poly-L-ornithine (20ug/ml) and laminin (5 μg/ml)-coated dishes and cultured in neural maintenance medium (NMM) consisting of NIM without LDN193189 and SB431542. When rosette structures were observed, 20 ng/ml bFGF was added for 4 days followed by a second split (1:3) using Dispase. Hereafter, the cells were split 1:3 by Accutase upon confluence. At days 21 and 35, the cells were fixed in 4% PFA for immunocytochemical analyses with neuron-specific antibodies (Supplementary table 1) and on day 80, recordings of intracellular calcium kinetics were performed. Cells in 96-well plates were incubated for 1h at RT with the fluorescent calcium indicator, Calcium 5 (Molecular Devices, Sunnyvale, CA, USA) dissolved in Hanks Balanced Salt Solution (HBSS; Life Technologies). Following loading, recordings were performed with an FDSS 7000 fluorescence kinetics plate reader (Hamamatzu Photonics K.K., Hamamatsu city, Japan). The excitation wavelength was 480 nm; the emission wavelength was 540 nm and the sampling frequency 1Hz.